Nuclear Physics A462 (1987) 252–268
North-Holland, Amsterdam

MULTIPOLE MOMENTS OF RARE-EARTH NUCLEI IN THE GENERATOR COORDINATE METHOD

B. NERLO-POMORSKA[1], K. POMORSKI[1], M. BRACK and E. WERNER

University of Regensburg, D-8400 Regensburg, W. Germany

Received 13 June 1986

Abstract: The collective multipole moment operators $\hat{Q}_\lambda^{\text{coll}}$ are constructed within the generator coordinate method (GCM) in gaussian overlap approximation (GOA). BCS wave functions are used as the generator functions. The Nilsson single-particle plus pairing hamiltonian is employed in this paper. When constructing the collective hamiltonian, the potential energies are evaluated by the Strutinsky shell correction method and the mass parameters are obtained by the GCM+GOA or the cranking model.

The kinetic and zero-point corrections to $\hat{Q}_\lambda^{\text{coll}}$ are found not to influence the mean values of the multipole moments by more than 1%. The GCM multipole moments are in good agreement with experimental data.

1. Introduction

The theoretical electric multipole, especially quadrupole, moments of nuclei were usually too small in comparison with the experimental data [e.g. ref. [1])]. These calculations were based on the assumption that a nucleus has a definite equilibrium deformation corresponding to the minimum of its potential energy.

In macroscopic models, the multipole moments are usually obtained from the charge density assuming a uniform or a Fermi function, integrated at the equilibrium point in deformation space. In a microscopic formulation one obtains the mean values of the multipole moment operators between the many-body wave functions, usually BCS functions, also at the equilibrium point.

In such calculations the dynamical vibrations of the nuclear surface are not taken into account.

In ref. [2]) an approximate estimate of the dynamical effects was proposed based on the Born–Oppenheimer assumption. First the expectation values of the multipole moment operators are calculated on a wide grid of deformation points. Then a folding is performed over the collective deformation variables with the square of the collective wave function, which is obtained by diagonalizing the collective hamiltonian. The latter is built with cranking mass parameters and a Strutinsky type potential energy surface. That rough method gives promising results improving the quadrupole moments by about 3% towards experimental data. The dynamical effects [2,3]) are especially large when calculating the potentials with the so-called

[1] On leave from the M.C.S. University, Department of Theoretical Physics, 20031 Lublin, Poland.

simple consistency condition [2]). This ensures the agreement between the single-particle and liquid-drop shapes in the Strutinsky method [4]), because in this case the potential energy surface is flatter around the minimum.

Nevertheless, a more complete and rigorous theory including the kinetic and zero-point corrections to the collective multipole moment operators seems necessary.

One convenient dynamical theory which gives such corrections is the generator coordinate method (GCM) with the gaussian approximation (GOA) for the overlap of generating functions [5]).

In ref. [6]) the multidimensional collective hamiltonian was derived within the GCM in the extended GOA. In the framework of this formalism not only the hamiltonian but also every hermitian operator, acting in the space of the single-particle coordinates, can be projected into the collective subspace $\{a\}$. We have used this method to construct the collective multipole moment operators in sect. 2 of this paper. In sect. 3 the parameters of the calculation for the lighter even-even rare earth nuclei are described and the results for their multipole moments are discussed.

2. Derivation of the collective multipole moment operators

The monopole, quadrupole and hexadecapole moment operators acting in the single-particle space of nucleon coordinates $\{r, \theta, \varphi\}$ are defined, respectively, by

$$\hat{Q}_0 = r^2\,, \qquad \hat{Q}_2 = 2r^2 P_2(\cos\theta)\,, \qquad \hat{Q}_4 = 2r^4 P_4(\cos\theta)\,, \tag{1}$$

where P_λ are the Legendre polynomials. We are starting from a set of many-body wave functions $|a\rangle$, depending on the single particle coordinates x and parametrically on the collective deformation parameters $\{a\}$: $|a\rangle = |x; a\rangle$. From now on set $\{a\}$ is denoted as the generator function. Now we can build the approximate collective wave function

$$|\psi(x)\rangle = \int_{-\infty}^{+\infty} f(a)|a\rangle \,\mathrm{d}a\,. \tag{2}$$

The weights $f(a)$ are obtained here in the extended gaussian approximation (GOA) of the generator function overlap $\langle a|a'\rangle$ [ref. [6])]. The average value of the multipole moment in the state $|\psi\rangle$ is then

$$\langle\psi|\hat{Q}_\lambda|\psi\rangle = \int_{-\infty}^{+\infty}\int_{-\infty}^{+\infty} f^*(a)\,\frac{\langle a|\hat{Q}_\lambda|a'\rangle}{\langle a|a'\rangle}\,\langle a|a'\rangle f(a')\,\mathrm{d}a\,\mathrm{d}a'\,. \tag{3}$$

The overlap $\langle a|a'\rangle$ carries the main dependence on the deformation difference $a - a'$ while the reduced overlap function

$$q_\lambda \equiv \frac{\langle a|\hat{Q}_\lambda|a'\rangle}{\langle a|a'\rangle} \tag{4}$$

can be expanded in a Taylor series around the deformation point $\frac{1}{2}(a+a')$. After calculating the expansion coefficients and assuming that the overlap can be transformed into a Gauss function [7]), we get the average value of the multipole moments in the collective state as

$$\langle\psi|\hat{Q}_\lambda|\psi\rangle=\int_{-\infty}^{+\infty}\Phi^*(a)\hat{Q}_\lambda^{\mathrm{coll}}\Phi(a)\sqrt{\det\gamma}\,\mathrm{d}a\,. \tag{5}$$

The functions $\Phi(a)$ are the eigenfunctions of the collective hamiltonian $\hat{\mathscr{H}}_{\mathrm{coll}}$; $\{\gamma\}$ is the width tensor of the generator function overlap

$$\gamma_{kl}=\langle a|\frac{\overleftarrow{\partial}}{\partial a_k}\frac{\vec{\partial}}{\partial a_l}|a\rangle\,. \tag{6}$$

The collective multipole moment operator contains kinetic and potential terms

$$\hat{Q}_\lambda^{\mathrm{coll}}=\hat{Q}_\lambda^{\mathrm{T}}+\hat{Q}_\lambda^{\mathrm{V}}\,, \tag{7}$$

where

$$\hat{Q}_\lambda^{\mathrm{T}}=\frac{1}{2\sqrt{\det\gamma}}\frac{\partial}{\partial a_i}\sqrt{\det\gamma}\,{}^\lambda\mathscr{M}_{ij}^{-1}\frac{\partial}{\partial a_j}\,. \tag{8}$$

The "multipole inertias" $\{{}^\lambda\mathscr{M}\}$ are

$${}^\lambda\mathscr{M}_{ij}^{-1}=\tfrac{1}{2}\gamma_{ik}^{-1}\left(2_\kappa q_l^\lambda-\frac{\partial}{\partial a_k}q_l^\lambda+\Gamma_{kl}^m q_m^\lambda\right)\gamma_{ij}^{-1}\,. \tag{9}$$

Here $\{\Gamma^m\}$ are the Christoffel symbols

$$\Gamma_{kl}^m=\tfrac{1}{2}\gamma_{m\tau}^{-1}\left(\frac{\partial\gamma_{k\tau}}{\partial a_l}+\frac{\partial\gamma_{l\tau}}{\partial a_k}-\frac{\partial\gamma_{kl}}{\partial a_\tau}\right). \tag{10}$$

The ${}_\kappa q_l^\lambda$ and q_k^λ are the following matrix elements of $\hat{Q}_\lambda$ taken between the derivatives of the generator functions:

$$q_k^\lambda\equiv\langle a|\hat{Q}_\lambda\frac{\vec{\partial}}{\partial a_k}|a\rangle\,, \tag{11}$$

$${}_\kappa q_l^\lambda\equiv\langle a|\frac{\overleftarrow{\partial}}{\partial a_k}\hat{Q}_\lambda\frac{\vec{\partial}}{\partial a_l}|a\rangle-\langle a|\hat{Q}_\lambda|a\rangle\langle a|\frac{\overleftarrow{\partial}}{\partial a_k}\frac{\vec{\partial}}{\partial a_l}|a\rangle\,. \tag{12}$$

The potential term Q_λ^{v} of $Q_\lambda^{\mathrm{coll}}$ consists of the mean value of $\hat{Q}_\lambda$ evaluated between generator functions and the so-called zero-point correction $\mathring{q}_\lambda$

$$\hat{Q}_\lambda^{\mathrm{v}}=\langle a|\hat{Q}_\lambda|a\rangle-\mathring{q}_\lambda\,, \tag{13}$$

where

$$\mathring{q}_\lambda\equiv\tfrac{1}{2}\gamma_{ij}^{-1}\,{}_iq_j^\lambda\,. \tag{14}$$

In our calculations the deformation dependent BCS functions are taken as generator functions

$$|a\rangle = \prod_{\nu>0} (u_\nu + v_\nu c_\nu^+ c_\nu^+)|0\rangle , \tag{15}$$

where $|\nu\rangle$ are the single particle states and c_ν^+ the particle creation operators. The generator function corresponds to the mean-field hamiltonian, taken to be of Nilsson type here, with the residual pairing interaction strength G:

$$\hat{H} = \sum_{\nu>0} E_\nu \alpha_\nu^+ \alpha_\nu + \sum_{\nu>0} 2e_\nu v_\nu^2 - \Delta^2/G - G \sum_{\nu>0} v_\nu^4 . \tag{16}$$

Here $\alpha_\nu^+(\alpha_\nu)$ are the usual BCS quasiparticle creation (annihilation) operators, $E_\nu = \sqrt{(e_\nu - \Lambda)^2 + \Delta^2}$ the quasiparticle energies, and e_ν the single-particle (Nilsson) levels. The Fermi surface Λ, energy gap Δ and occupation factors u_ν, v_ν obey the usual set of BCS equations. Using first-order perturbation theory, one gets for $\partial|a\rangle/\partial a_i$ the expression

$$\frac{\partial}{\partial a_i}|a\rangle = \sum_{\mu\nu>0} (p_i)_{\mu\nu} \alpha_\mu^+ \alpha_\nu^+ |a\rangle , \tag{17}$$

where the matrix $\{p_i\}$ is defined by

$$(p_i)_{\mu\nu} = \frac{\langle\mu|\partial H/\partial a_i|\nu\rangle}{E_\mu + E_\nu}(u_\mu v_\nu + v_\nu u_\mu) + \left(\frac{\Delta}{2E_\nu^2}\frac{\partial \Lambda}{\partial a_i} + \frac{e_\nu - \Lambda}{2E_\nu^2}\right)\delta_{\mu\nu} . \tag{18}$$

Using this formula and applying the Bogolubov transformation to the operators $\hat{Q}_\lambda$ (1), one gets the explicit form of eqs. (6), (11), (12):

$$\gamma_{kl} = \sum_{\mu,\nu>0} (p_k)^*_{\mu\nu} (p_l)_{\nu\mu} , \tag{18}$$

$$q_l^\lambda = \sum_{\mu,\nu>0} \langle\mu|\hat{Q}_\lambda|\nu\rangle (u_\mu v_\nu + u_\nu v_\mu)(p_l)_{\nu\mu} , \tag{19}$$

$${}_k q_l^\lambda = 2 \sum_{\mu\nu\tau>0} (p_l)^*_{\tau\mu} \langle\mu|\hat{Q}_\lambda|\nu\rangle (u_\nu u_\mu - v_\nu v_\mu)(p_l)_{\nu\tau} . \tag{20}$$

To get the mean values of the multipole moment operators (5), we need good collective wave functions $\Phi(a)$. The collective hamiltonian is constructed in the following way. We calculate the nuclear potential energy as a function of the deformation parameters using the Strutinsky prescription [4]). Then the mass parameters ${}^{\mathrm{GCM}}B$ are obtained in the GCM from the formula

$$({}^{\mathrm{GCM}}B^{-1})_{ij} = \tfrac{1}{2}\gamma_{ik}^{-1}\, {}_k h_l \gamma_{lj}^{-1} , \tag{21}$$

where

$${}_k h_l \equiv \langle a|\frac{\partial}{\partial a_k} H \frac{\partial}{\partial a_l}|a\rangle = \sum_{\mu,\nu>0} (p_k)^*_{\mu\nu}(E_\mu + E_\nu)(p_l)_{\nu\mu} . \tag{22}$$

For comparison, we calculate also the cranking mass parameters ^{cr}B to get the dynamical multipole moments as in refs. [2,3]):

$$(^{cr}B)_{ij} = 2 \sum_{\mu\nu>0} (p_i)^*_{\mu\nu}(E_\mu + E_\nu)^{-1}(p_j)_{\nu\mu} . \tag{23}$$

3. Results

The calculation is performed in the lighter region of even-even rare-earth nuclei. The quadrupole ($a_1 = \varepsilon$) and hexadecapole ($a_2 = \varepsilon_4$) deformations are used as the generator variables. The $A \sim 165$ set of the Nilsson potential parameters is taken from [ref. [8])]. The pairing force strength is $GN^{2/3} = 0.29\hbar\omega_0$ [ref. [9])] and $2\sqrt{15\mathcal{N}}$ levels are included in the BCS sum equations. ($\mathcal{N} = Z(N)$ when protons (neutrons) are discussed.) The microscopic calculations are performed on the deformation grid $\varepsilon = -0.2$ (0.05) 0.4, $\varepsilon_4 = -0.12$ (0.04) 0.16. Eight major shells for protons and nine for neutrons are taken when diagonalizing the Nilsson single particle hamiltonian. The coupling between the shells through the hexadecapole term is included. The Strutinsky smearing parameter is $\gamma = 1\hbar\omega_0$ [ref. [4])]. The macroscopic part of the potential energy is assumed to be the liquid drop energy. Results obtained with the droplet model energy differ only slightly from the ones presented here.

In fig. 1 we show a typical map (for ^{166}Er) of the potential energy surface V in the rare-earth region of nuclei. The deformation parameters are ε and ε_4. The deformation energy for ^{166}Er is about 8 MeV; the equilibrium point, denoted by a cross is situated at $\varepsilon = 0.264$, $\varepsilon_4 = 0.014$. Up to now, the theoretical multipole moments

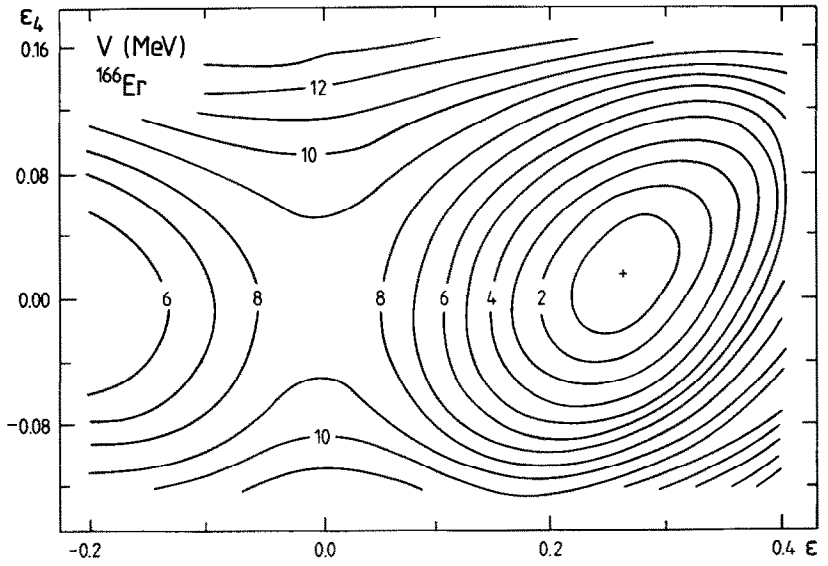

Fig. 1. The potential energy surface V on the ε, ε_4 plane of ^{166}Er. The points of equal energy signed in MeV are joined by solid lines. A cross corresponds to the equilibrium point.

have been calculated only at this point. We improve and complete the study by using the whole two-dimensional function $V(\varepsilon, \varepsilon_4)$ as the collective potential.

In fig. 2 we see the behaviour of the monopole moment $Q_0 = \langle a|r^2|a\rangle$ of ^{166}Er as function of the ε, ε_4 deformations. Q_0 depends mainly on ε. At the equilibrium point it is equal to 18.92 b.

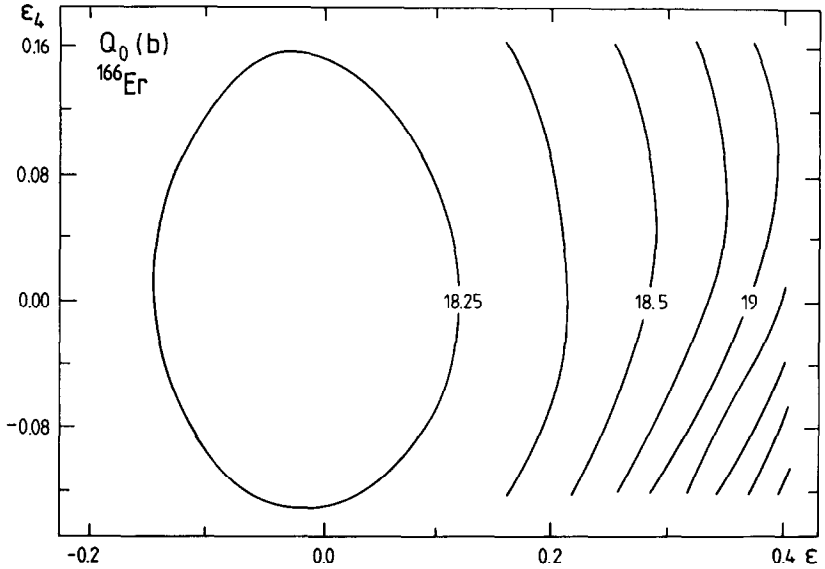

Fig. 2. The charge monopole moments $Q_0(\varepsilon, \varepsilon_4)$ of the ^{166}Er.

The quadrupole moment $Q_2 = \langle a|\hat{Q}_2|a\rangle$ of ^{166}Er is shown in fig. 3. It has also a weak dependence on ε_4. Its equilibrium value is 7.2 b.

The hexadecapole moment $Q_4 = \langle a|\hat{Q}_4|a\rangle$ depends stronger on ε_4 and is equal to 0.49 b^2 at the equilibrium point as can be seen in fig. 4 for ^{166}Er.

The two-dimensional functions $Q_\lambda(\varepsilon, \varepsilon_4)$ have been used to calculate the dynamical moments in refs. [2,5]). In our calculation they consititute the main part of the potential multipole moment operator (13) and are improved by the zero-point corrections illustrated for ^{166}Er in figs. 5 and 6. These corrections are small. They oscillate around zero with an amplitude of the order of 0.25 b for $\mathring{q}_2$ (fig. 5) and 0.125 b^2 for $\mathring{q}_4$ (fig. 6). We find that the zero-point corrections (12) thus do not influence the multipole moments by more than 1%.

To get the collective multipole operators and inertias, or the mass parameters, we need also the overlap width $\{\gamma\}$ (6), (18). It is illustrated for ^{166}Er in figs. 7–9.

In fig. 7, $\gamma_{\varepsilon\varepsilon}$ for ^{166}Er is drawn. It oscillates around $220\hbar^2$ and depends strongly on both ε and ε_4 deformations.

The $\gamma_{\varepsilon\varepsilon_4}$ values, shown in fig. 8, are smaller and oscillate around 0 with an amplitude of about $90\hbar^2$ for ^{166}Er which is smaller than $\gamma_{\varepsilon\varepsilon}$ and depends more weakly on ε_4.

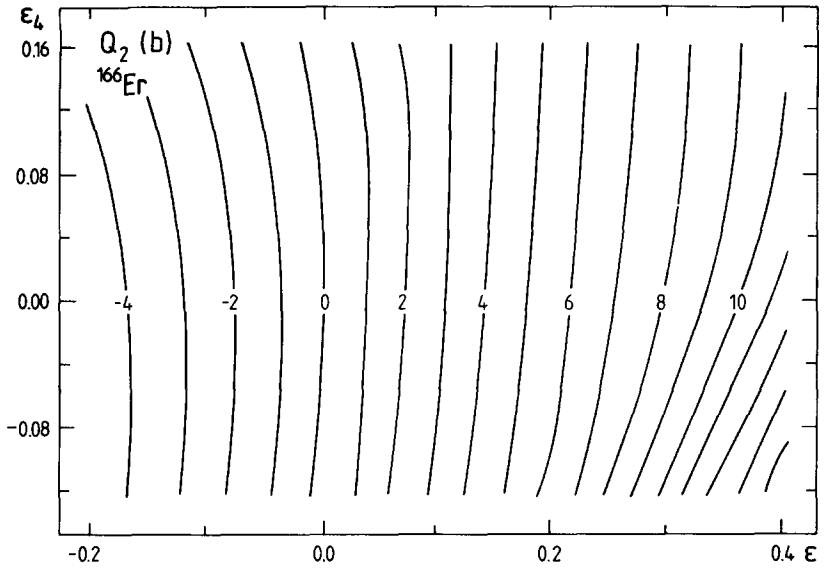

Fig. 3. The electric quadrupole moments $Q_2(\varepsilon, \varepsilon_4)$ of the ^{166}Er.

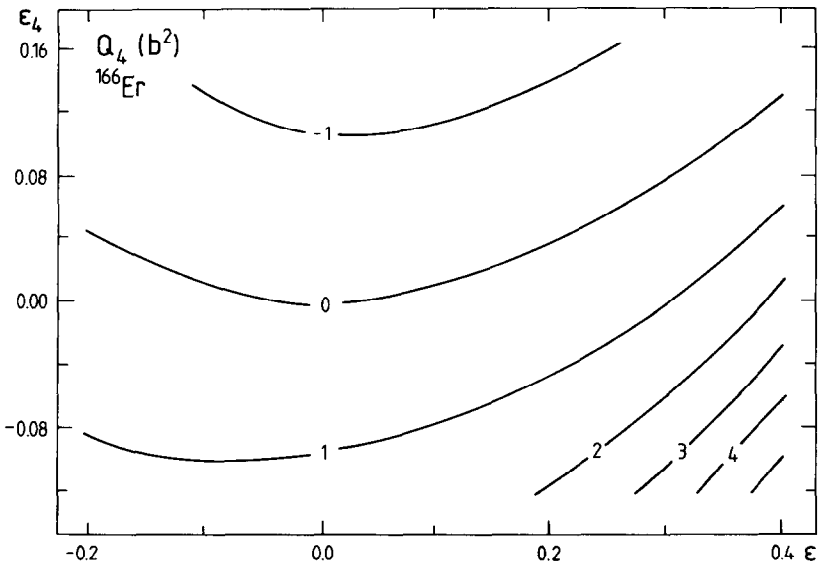

Fig. 4. The electric hexadecapole moments $Q_4(\varepsilon, \varepsilon_4)$ of ^{166}Er.

All the $\{\gamma\}$ elements are contained in the denominators of the inversed multipole inertias $\{\mathcal{M}^{-1}\}$ and put them rapidly to 0.

The map of $\mathcal{M}^{-1}_{\varepsilon\varepsilon}$ is drawn for ^{166}Er in fig. 10. For all ε, ε_4 points it is at order of magnitude 10^{-5} b. Similar results are obtained from the $M^{-1}_{\varepsilon\varepsilon_4}$ and $M^{-1}_{\varepsilon_4\varepsilon_4}$. All the elements depend rather weakly on the deformation. As their derivatives occurring

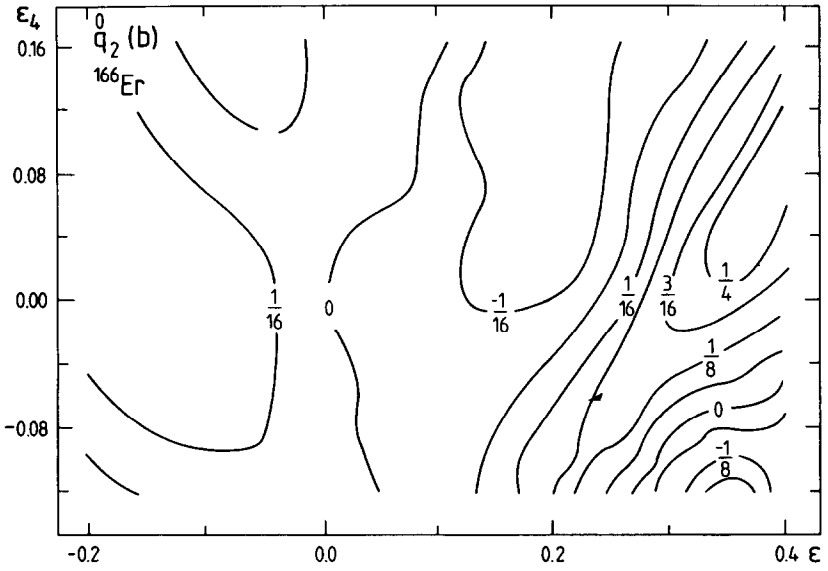

Fig. 5. The zero-point correction $\mathring{q}_2(\varepsilon, \varepsilon_4)$ to the potential quadrupole moment operator of ^{166}Er.

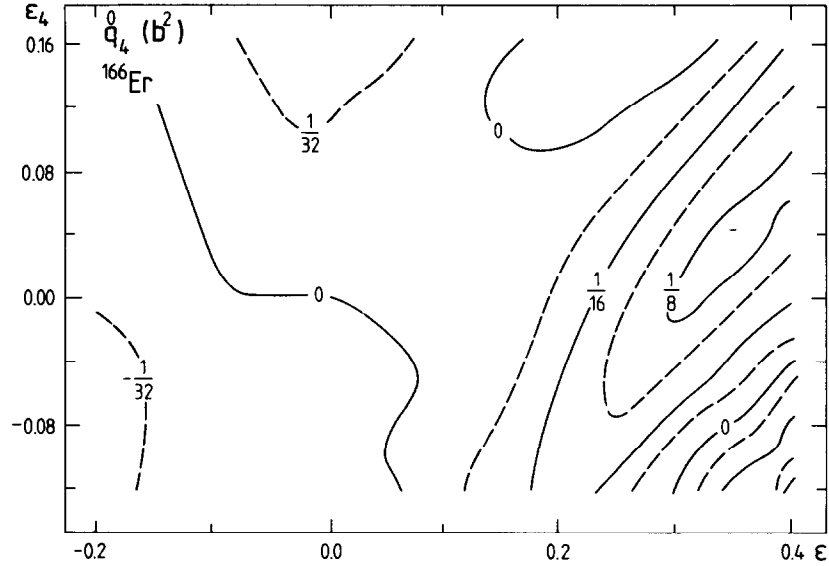

Fig. 6. The zero-point correction $\mathring{q}_4(\varepsilon, \varepsilon_4)$ to the potential hexadecapole moment operator of ^{166}Er.

in $\hat{Q}^{\mathrm{T}}_{\lambda}$ (8) are small, the kinetic part of the multipole moment operators practically vanishes. This means that the largest influence of the dynamical effects is coming from the collective wave function by the collective hamiltonian. In refs. [2,3]) it was built from cranking mass parameters $\{^{\mathrm{cr}}B\}$; we use $\{B^{\mathrm{GCM}}\}$ (21) here.

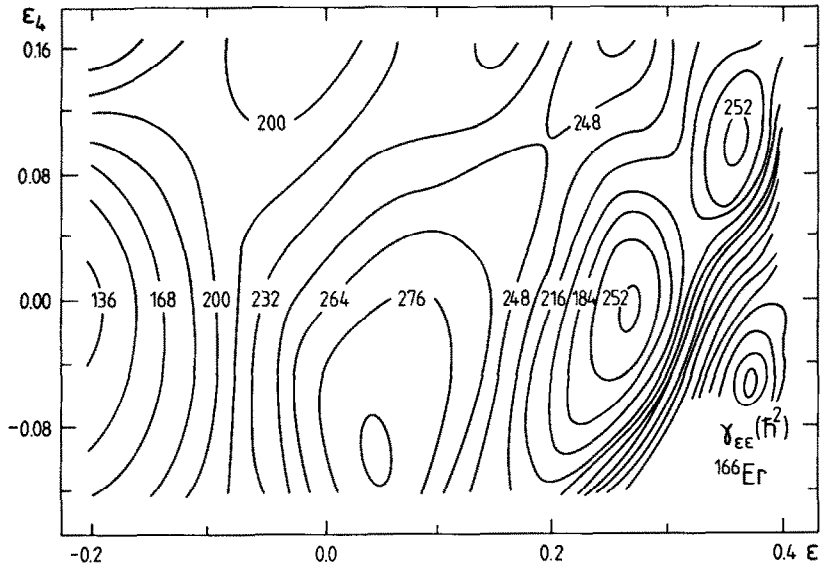

Fig. 7. The overlap width $\gamma_{\varepsilon\varepsilon}(\varepsilon, \varepsilon_4)$ of ^{166}Er.

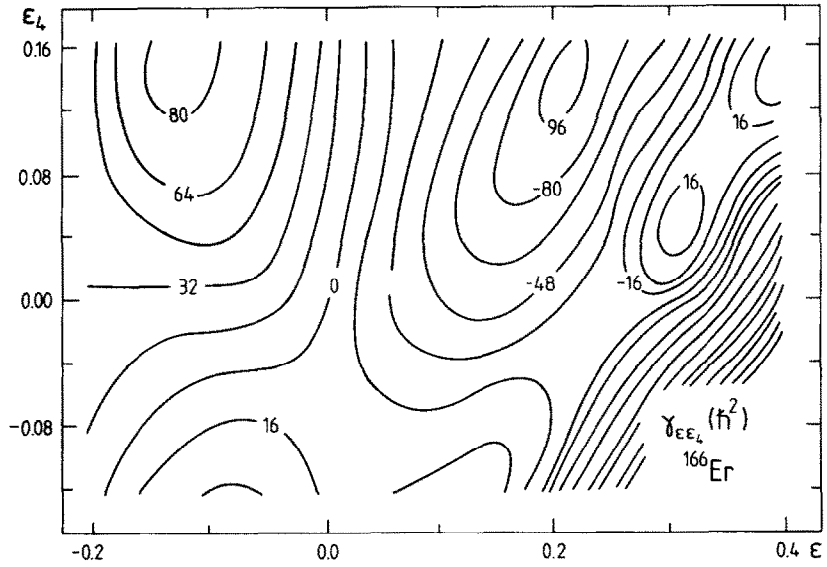

Fig. 8. The overlap width $\gamma_{\varepsilon\varepsilon_4}(\varepsilon, \varepsilon_4)$ of ^{166}Er.

In fig. 11 a map of B^{cr} (23) for ^{166}Er is shown. We can compare it with the B^{GCM} drawn for ^{166}Er in fig. 12. The dependence on the deformation is weaker here and B^{GCM} are on the average smaller by 30% than B^{cr}.

The nondiagonal parameters $B^{\mathrm{GCM}}_{\varepsilon\varepsilon_4}$ of ^{166}Er, drawn in fig. 13, oscillate around 0. In fig. 14 the parameters $B^{\mathrm{GCM}}_{\varepsilon_4\varepsilon_4}$ are shown.

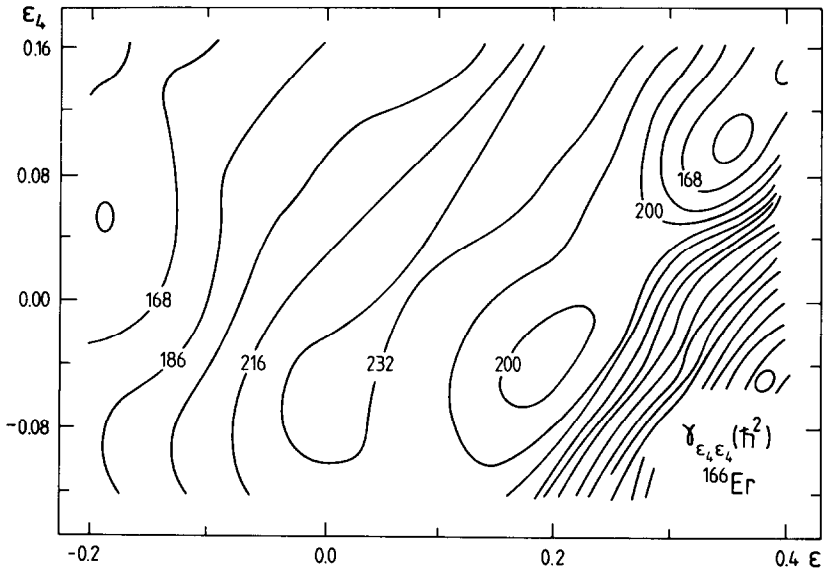

Fig. 9. The overlap with $\gamma_{\varepsilon_4\varepsilon_4}(\varepsilon, \varepsilon_4)$ of ^{166}Er.

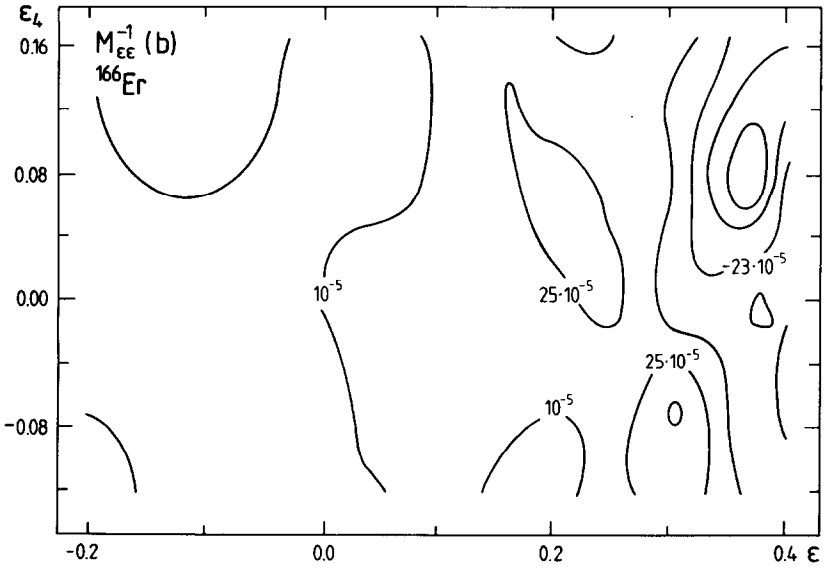

Fig. 10. The inversed multipole moment inertia $M^{-1}_{\varepsilon\varepsilon}(\varepsilon, \varepsilon_4)$ of ^{166}Er.

All the maps 5-14 show a sharp increase of the illustrated functions for large deformations because the potential energy of ^{166}Er (fig. 1) is also very steep there.

The collective wave functions obtained by the digonalization of the collective hamiltonian with cranking (fig. 15) and GCM (fig. 16) mass parameters for ^{166}Er

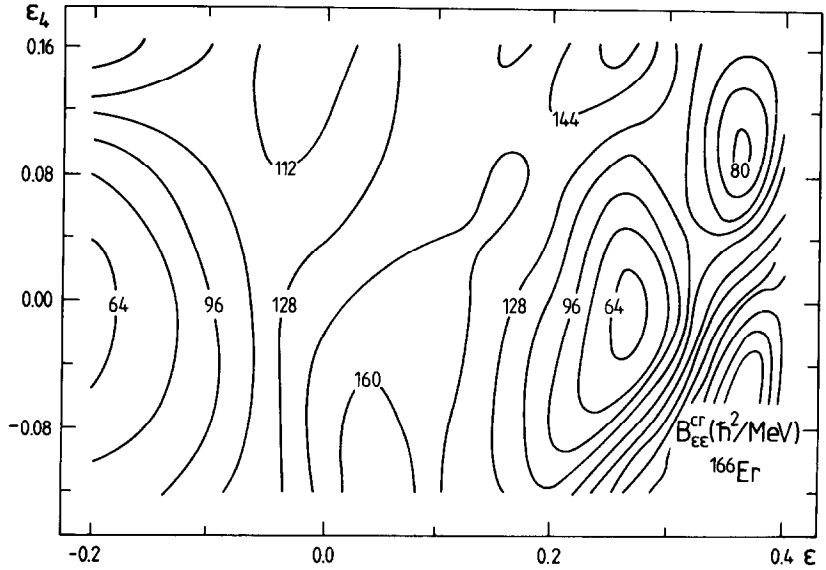

Fig. 11. The cranking mass parameter $B^{cr}_{\varepsilon\varepsilon}(\varepsilon, \varepsilon_4)$ of ^{166}Er.

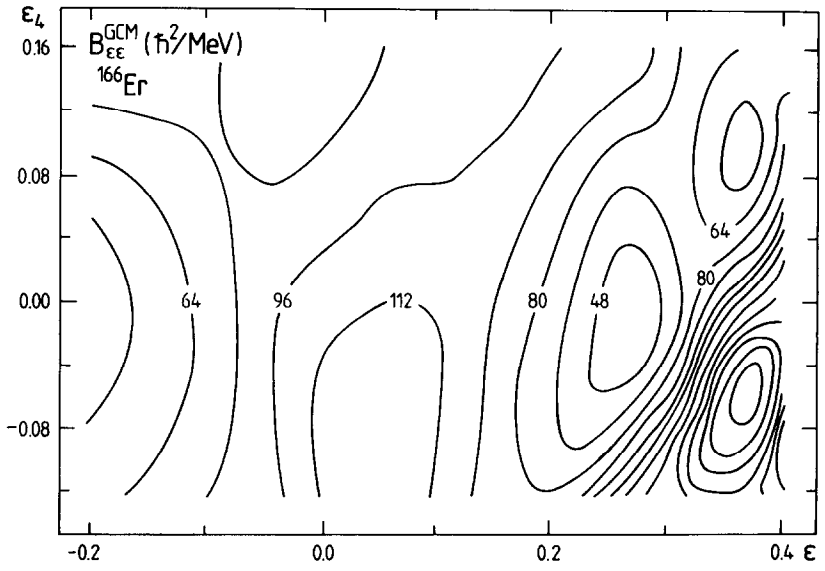

Fig. 12. The GCM mass parameter $B^{GCM}_{\varepsilon\varepsilon}(\varepsilon, \varepsilon_4)$ of ^{166}Er.

do not differ very much from each other. The B^{GCM} (fig. 16) is flatter in both ε and ε_4 directions, so that the dynamical effects should be larger in this case.

Nevertheless we observe that the main influence of the dynamics is on the potential part of the multipole moment operators $\langle a|\hat{Q}_\lambda|a\rangle$, even without the zero-point

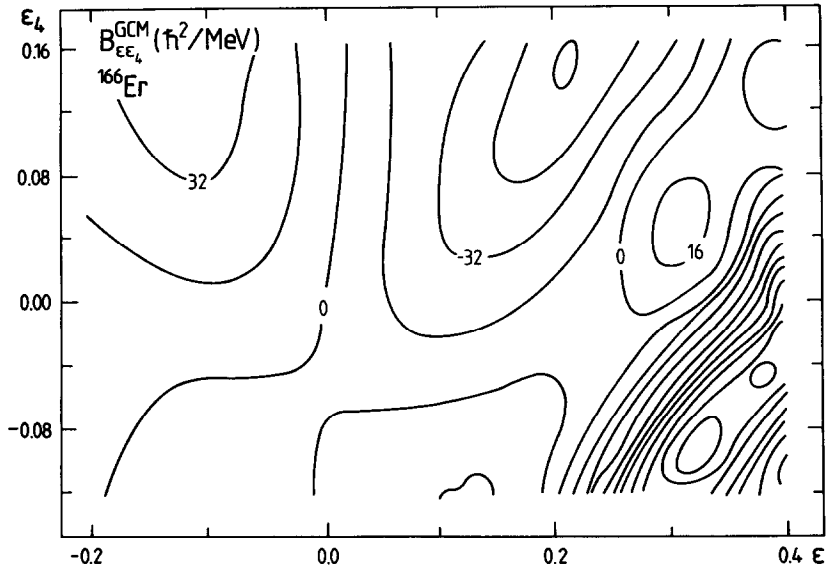

Fig. 13. The GCM mass parameter $B^{GCM}_{\varepsilon\varepsilon_4}(\varepsilon, \varepsilon_4)$ of ^{166}Er.

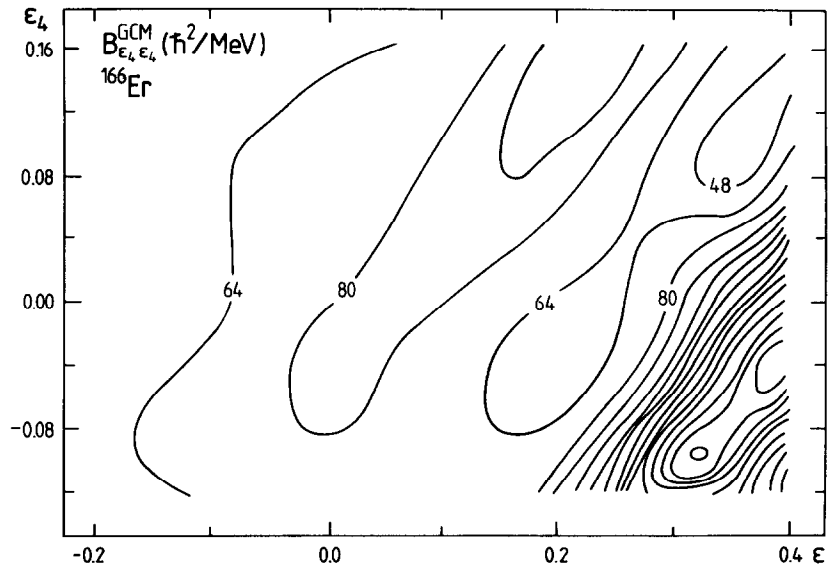

Fig. 14. The GCM mass parameter $B^{GCM}_{\varepsilon_4\varepsilon_4}(\varepsilon, \varepsilon_4)$ of ^{166}Er.

corrections $\mathring{q}_\lambda$. The multipole moments calculated only with this term

$$Q_\lambda \cong \int_{-\infty}^{+\infty} \Phi^*(a)\langle a|\hat{Q}_\lambda|a\rangle\Phi(a)\sqrt{\det\gamma}\,\mathrm{d}a\,, \tag{24}$$

do not differ more than 1% from those obtained by formula (5). It means that the main advantage of applying the GCM to the calculation of multipole moments

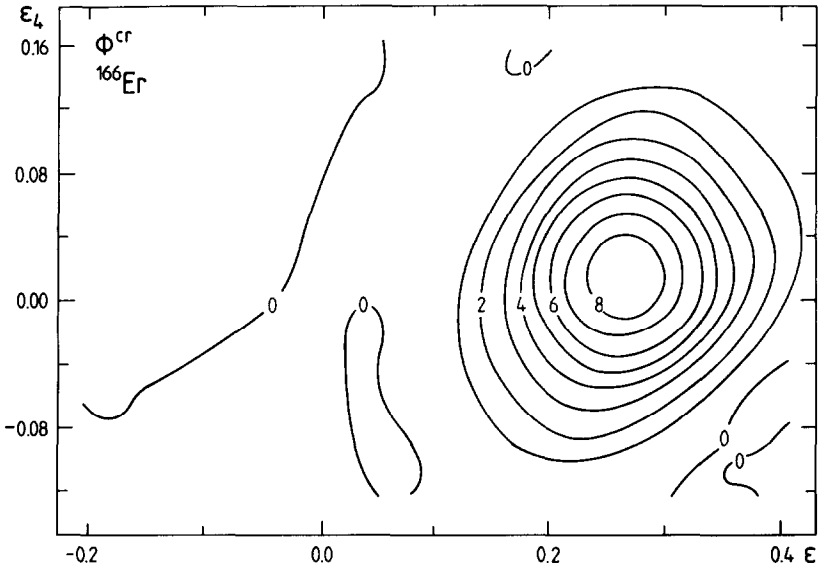

Fig. 15. The collective wave function $\Phi^{cr}(\varepsilon, \varepsilon_4)$ of ^{166}Er calculated with the cranking mass parameters.

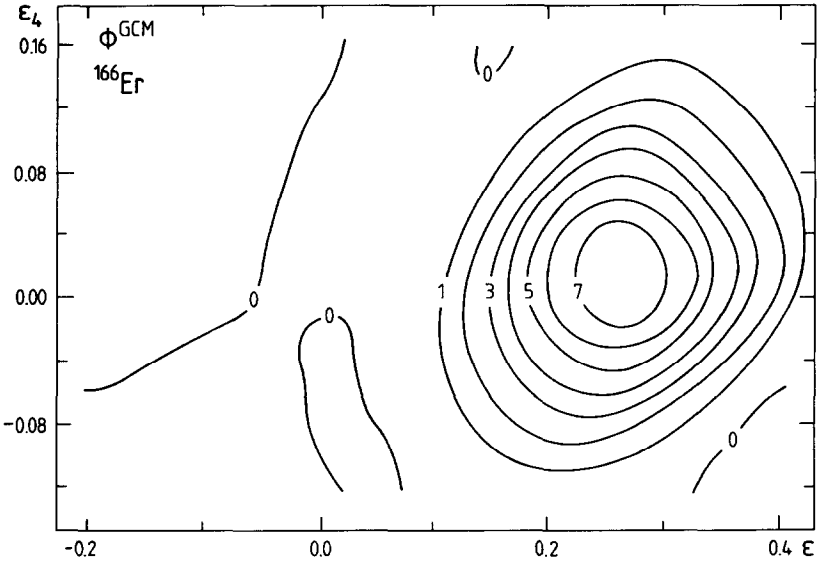

Fig. 16. The collective wave function $\Phi^{GCM}_{(\varepsilon,\varepsilon_4)}$ of ^{166}Er calculated with the GCM mass parameters.

comes through the collective wave functions obtained from the collective hamiltonian with GCM mass parameters.

The final multipole moments of the lighter even-even rare-earth nuclei are drawn in figs. 17-19.

In fig. 17 we can see the variation of the mean square charge radius

$$\delta\langle r^2\rangle_{N-2,N} = \langle r^2\rangle_{N,Z} - \langle r^2\rangle_{N-2,Z} \tag{25}$$

as function of the neutron number N for several pairs of rare-earth nuclear isotopes. The theoretical results are compared with the experimental data taken from ref. [10]) (crosses) and [11]) (squares). For the lighter Nd-Sm nuclei the results for $N = 90$ are well reproduced. For heavier Dy-Hf nuclei, a systematic error of about 1 fm^2 occurs.

The quadrupole moments are shown in fig. 18. The experimental data (crosses) taken from refs. [12-14]) agree well (to 3%) with the theoretical results. Nevertheless the agreement is not much better than in ref. [3]). We would like to stress that in our calculation no other effects like renormalization of the liquid drop or potential energy are included, because only the dynamical corrections of GCM are of interest for us.

The hexadecapole moments of rare-earth nuclei are drawn in fig. 19. The experimental data (crosses) are taken from refs. [12,14]). The discrepancies are sometimes larger than experimental errors (to 30%).

The comparison between the experimental data and our theoretical results demands some more explanation. Usually the weighted average values from various experiments are treated as being the proper results [12,14]). Most of the data are taken from the reduced transition probabilities $B(E\lambda)$ between the ground state bands

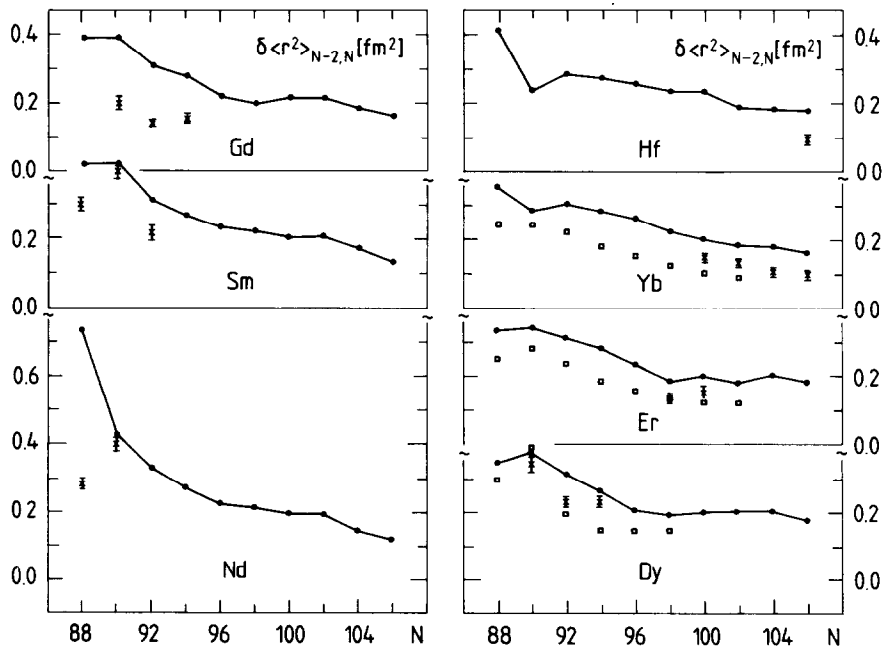

Fig. 17. The variations of the charge mean square radius $\delta\langle r^2\rangle$ for pairs of rare-earth nuclear isotopes as functions of the neutron number N. The crosses denote experimental data from ref. [10]), the squares the ones from ref. [11]).

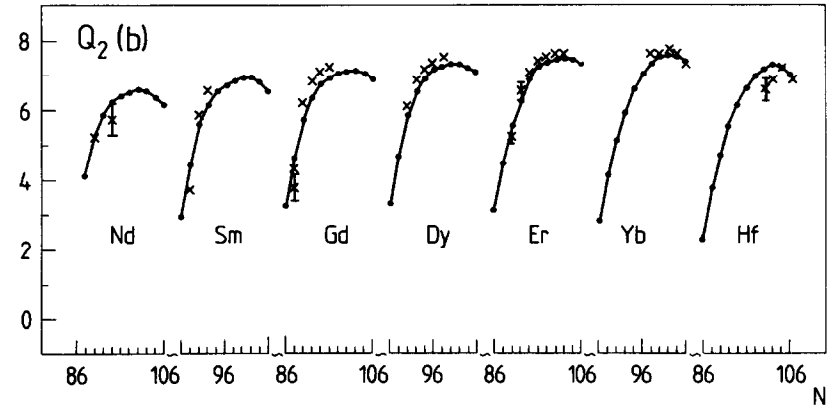

Fig. 18. The quadrupole electric moments of the light rare-earth even-even nuclei. The crosses denote experimental data [12,13]).

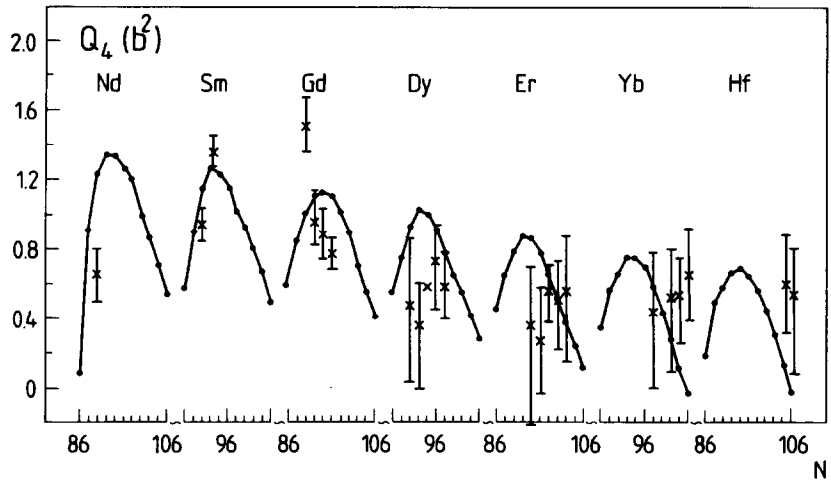

Fig. 19. The hexadecapole electric moments of the light rare-earth even-even nuclei. The crosses denote experimental data [12,14]).

($K=0$) [ref. [15])]. The probabilities $B(\mathrm{E}\lambda)$ are connected with the moments Q_λ by the simple relation

$$B(\mathrm{E}\lambda, \lambda^+ \to 0^+) = \frac{2\lambda+1}{16\pi} Q_\lambda^2 , \tag{26}$$

which can be derived within the rotational model of a nucleus. A better, model-independent, information about the multipole moments is given by the sum of transition probabilities from the various λ^+ states to the 0^+ ground state. We are thankful to Dr. J. Srebrny and G. Rohoziński for turning our attention to this

problem. Then we get

$$\sum_{\lambda^+} B(\mathrm{E}\lambda, \lambda^+ \to 0^+) = \sum_{\lambda^+} \sum_{\mu=-\lambda}^{\lambda} |\langle 0^+|\mathcal{M}(\mathrm{E}\lambda, \mu)|\lambda^+\rangle|^2$$

$$= \sum_{\mu=-\lambda}^{\lambda} \langle 0^+|\mathcal{M}^*(\mathrm{E}\lambda, \mu)\mathcal{M}(\mathrm{E}\lambda, \mu)|0^+\rangle$$

$$= \sqrt{\frac{2\lambda+1}{16\pi}} \sum_{\mu=-\lambda}^{\lambda} \langle 0^+|Q^*_{\lambda\mu} Q_{\lambda\mu}|0^+\rangle , \tag{27}$$

where $M(\mathrm{E}\lambda, \mu)$ is the electric multipole transition operator. In such a case the $\hat{Q}^2_\lambda$ operator rather than $\hat{Q}_\lambda$ should be projected onto the collective subspace. However, in order to apply the formula (27) one needs experimental information about the transition $\lambda^+ \to 0^+$ for all the excited states λ^+, which is difficult to measure. Nevertheless, a weighted average of experimental Q_λ values, containing the mixture of various measurements can be compared with the results of our theory, where $\hat{Q}_\lambda$ is projected onto the collective subspace.

We expect that the application of the QCM + GOA to the calculation of multipole moments can bring larger effects if a self-consistent mean field derived from a nucleon–nucleon force is used instead of the phenomenological Nilsson potential. The zero-point corrections to $\langle a|H|a\rangle$ then do not vanish, therefore changing the collective wave function. The dynamical effects would be also larger for lighter deformed nuclei than rare-earth nuclei with flatter potential energies around the equilibrium points.

Nevertheless we have proved that the method of calculation proposed in ref. [2]) is quite sufficient to estimate the dynamical effects in electric multipole moments.

4. Conclusions

The following conclusions can be drawn from our investigations.

1. The collective multipole moment operators obtained within GCM + GOA consist of the kinetic $\hat{Q}^{\mathrm{T}}_\lambda$ and the potential $\hat{Q}^{\mathrm{V}}_\lambda$ term with the zero-point vibrational correction $\mathring{q}_\lambda$.

2. The kinetic $\hat{Q}^{\mathrm{T}}_\lambda$ and zero-point $\mathring{q}_\lambda$ terms give not more than 1% corrections to the multipole moments.

3. The main part of the multipole moment operator $Q^{\mathrm{coll}}_\lambda$ is $\langle \mathrm{a}|\hat{\mathrm{Q}}_\lambda|\mathrm{a}\rangle$ and its average value evaluated with the collective wave functions is sufficient to calculate the multipole moments of nuclei.

4. The collective wave functions obtained with the GCM mass parameters give multipole moments which are 1% larger than those with cranking mass parameters.

5. The variations of the mean squared charge radius of rare-earth nuclear isotopes obtained from the GCM + GOA method are about 1 fm larger than the experimental data.

6. The electric quadrupole moments of rare-earth nuclei calculated by the GCM method are up to 5% smaller than the experimental data, for HF isotopes they become 2% larger.

7. The electric hexadecapole moments of rare-earth nuclei obtained with the GCM method differ up to 30% from the experimental data.

The first two authors are very grateful to the Institute for Theoretical Physics for warm hospitality during their stay at Regenburg University. Grants from Deutsche Forschungsgemeinschaft (DFG) and Gesellschaft für Schwerionenforschung (GSI) are also appreciated.

References

1) B. Nerlo Pomorska, Nucl. Phys. **A259** (1976) 481
2) B. Nerlo Pomorska and K. Pomorski, Z. Phys. **A309** (1983) 341
3) P. Rozmej, Nucl. Phys. **A445** (1985) 495
4) V.M. Strutinsky, Nucl. Phys. **A95** (1967) 420
5) P. Ring and P. Schuck, The nuclear many-body problem (Springer, Heidelberg, 1980)
6) A. Gózdź, K. Pomorski, M. Brack and E. Werner, Nucl. Phys. **A442** (1985) 26
7) A. Gózdź, Phys. Lett. **B152** (1985) 281
8) S.G. Nilsson, G.F. Tsang, A. Sobiczewski, Z. Szymański, S. Wycech, C. Gustafson, I.L. Lang, P. Möller and B. Nilsson, Nucl. Phys. **A131** (1969) 1
9) K. Bönnig, A. Sobiczewski and K. Pomorski, Acta. Phys. Polon. **B16** (1985) 393
10) F. Boem and P.L. Lee, Atomic Data and Nucl. Data Tables **14** (1974) 605
11) E.W. Otten, Proc. Int. School on heavy ions physics, Alushta, Crimea, USSR, April (1986)
12) K.E.G. Löbner, M. Vetter and V. Hönnig, Nucl. Data. Tables **A7** (1970) 495
13) A.S. Goldhaber and G. Scharff-Goldhaber, Phys. Rev. **C17** (1978) 1171
14) R.M. Ronningen, J.H. Hamilton, L. Varnvell, I. Lange, A.V. Ramagya, G. Gracia-Bermudez, W. Laurens, L.L. Riedinger, F.K. McGowan, P.H. Stelson, R-L. Robinson and J.L.C. Ford Jr., Phys. Rev. **C16** (1977) 2208
15) V.G. Soloviev, Theory of complex nuclei (Pergamon, Frankfurt, 1976)